Volume density maps of the 862 nm DIB carrier and interstellar dust

Hints on the role of carbon-rich ejecta from AGB stars

Author: N. L. J. Cox, J. L. Vergely, and R. Lallement

Reporter: Yanan Cao

1. Introduction

- Diffuse interstellar bands (DIBs) consist of absorptions of various shapes and depths distributed in the optical and near-infrared spectra of distant objects. Catalogues of DIBs have been consistently expanding due to the accumulation of stellar spectra of rising quality, reaching more than 500 different features *(Fan et al. 2019)*.

- DIBs are omnipresent in the Universe*(Heckman & Lehnert 2000; Cordiner et al. 2011; Monreal-Ibero et al. 2015)*, which can be used to study the physicochemical conditions of the interstellar medium (ISM). **Their carriers have effectively remained unidentified** *(Cami & Cox 2014)*, and only a few carriers such as C_{60+} have been confirmed *(Foing & Ehrenfreund 1994; Campbell et al. 2015; Cordiner et al. 2019)*.

- The column densities of their carriers are known to be correlated with the amount of interstellar dust or gas *(Vos et al. 2011; Friedman et al. 2011)*.

- The local effective radiation field is affecting the relative abundances between different DIB carriers *(Vos et al. 2011)*. **Most DIB carriers become depleted in opaque regions, namely, towards the interior of dense interstellar clouds.** This is called the “skin effect.”

1. Introduction

- The 862 nm DIB is a broad band (FWHM of ~0.4 nm). Being spectrally close to ionized calcium lines commonly used to constrain the stellar parameters, its study benefits from stellar spectroscopic surveys using these stellar lines.
- Its study was recently boosted due to its presence in the spectral interval selected for the Radial Velocity Spectrometer (RVS), the high-resolution spectrometer on board Gaia. *(Gaia Collaboration, 2023b)*
- Maps of DIB equivalent widths (EWs) or absorption strengths have been presented for several DIBs based on ground surveys *(Kos et al. 2014; Baron et al. 2015; Zasowski et al. 2015)* and more recently on Gaia data *(Gaia Collaboration 2023b; Gaia Collaboration 2023a)*.
- **In this work, they build the first, large-scale, fully 3D map of a DIB carrier**, tracing it out to ~2000 pc from the Sun, and do the first comparisons between local values of DIB carriers and dust grains.

2. Data

- ❑Gaia DR3: includes DIB measurements for 463 486 sources
- ❑parallax error $<20\%$ (ePlx/Plx < 0.2); DIB quality flag = 0, 1, or 2 (qDIB < 3); $|z| < 400$ pc (only sources within 400 pc of the galactic plane); $r < 5000$ pc (only sources within 5 kpc of the Sun) → 202 340 sources
- ❑They attempted to exclude features at 861.6, 861.7, and 862.5 nm which are thought to be stellar lines masquerading as DIBs: filtering on λDIB (in nm): $862.52 < \lambda\mathrm{DIB} < 862.58$, $861.76 < \lambda\mathrm{DIB} < 861.78$, $861.66 < \lambda\mathrm{DIB} < 861.70$. → 175 578 sources

3. Methodology

- The reconstruction of the volume (3D) density of either interstellar dust grains producing the extinction or of DIB carriers is based on the inversion of a catalog of measured integrated values, that is, **as seen from the origin up to a given point (x, y, z) at a distance, d, the target star location.**

- They did not use individual DIB equivalent widths, but an average of many values made over spatial boxes. The size of the boxes depends on the resolution. For a 100-pc resolution reconstruction, boxes have a size of 100 × 100 × 100 pc.

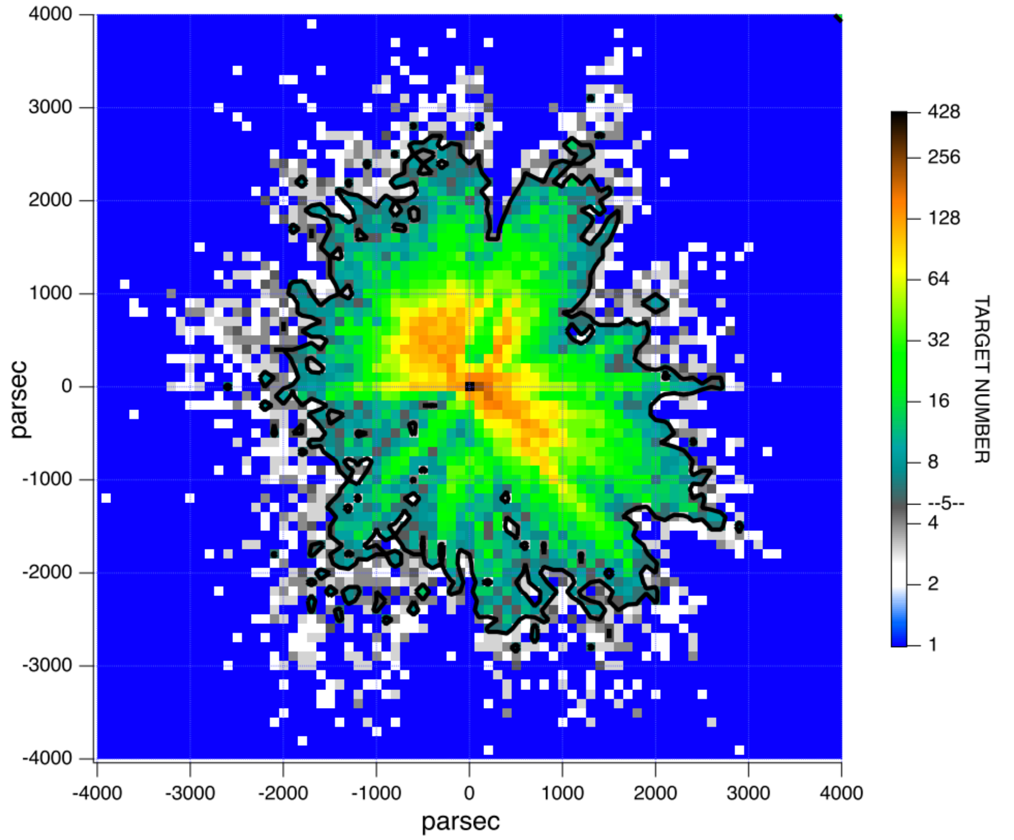

Fig. 1. Coverage of sources in the input catalog along the Galactic plane. The number of sources per 100^3 pc^3 cell is color-coded. All sources with abs(z) <50 pc are included. The limit of five targets per cell used in the statistical study is marked by a thick black line.

3. Methodology

- Beyond 2–3 kpc there are fewer objects, while the sampled volume increases exponentially. The reconstructed density cubes are cut off at 4 kpc.
- They set the limiting distance to the distance of the most distant distance bin with at least five stars. Beyond this bin, the accuracy of the map was severely hampered by the lack of input data.

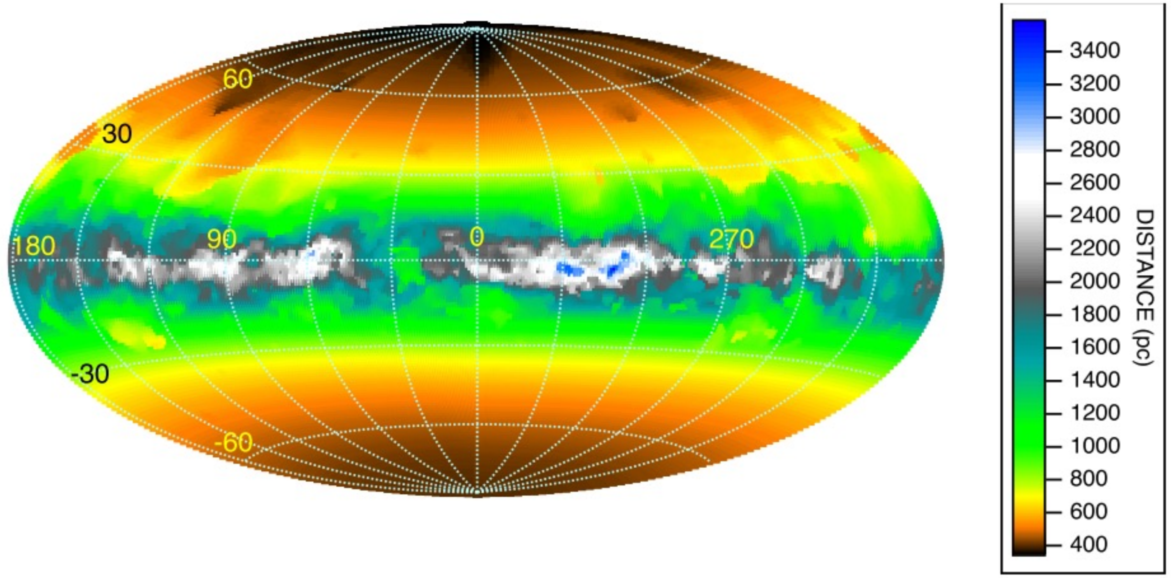

Fig. 2. Aitoff projection of the maximum reliable distance map for the DIB 3d reconstruction. Iso-Galactic longitudes and latitudes are drawn spaced by 30°. The Galactic Center ($l = 0$) is at the center and longitudes are increasing to the left. The reconstruction in the Galactic plane ($|b| < 15°$) has the highest fidelity.

4. Results

862.1 nm DIB carrier volume density

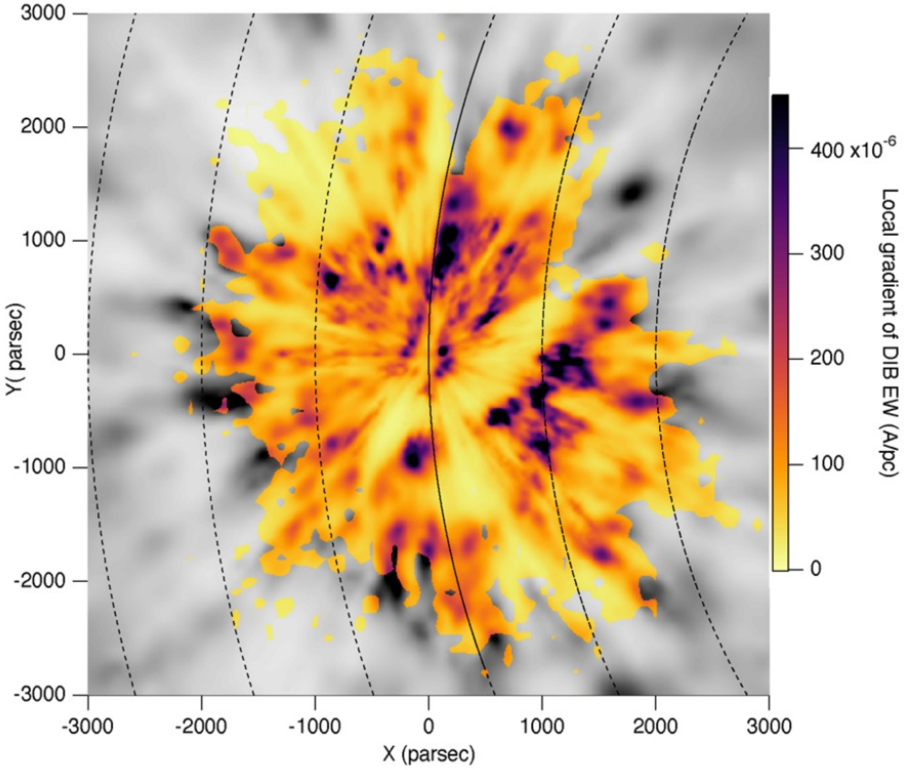

Extinction volume density

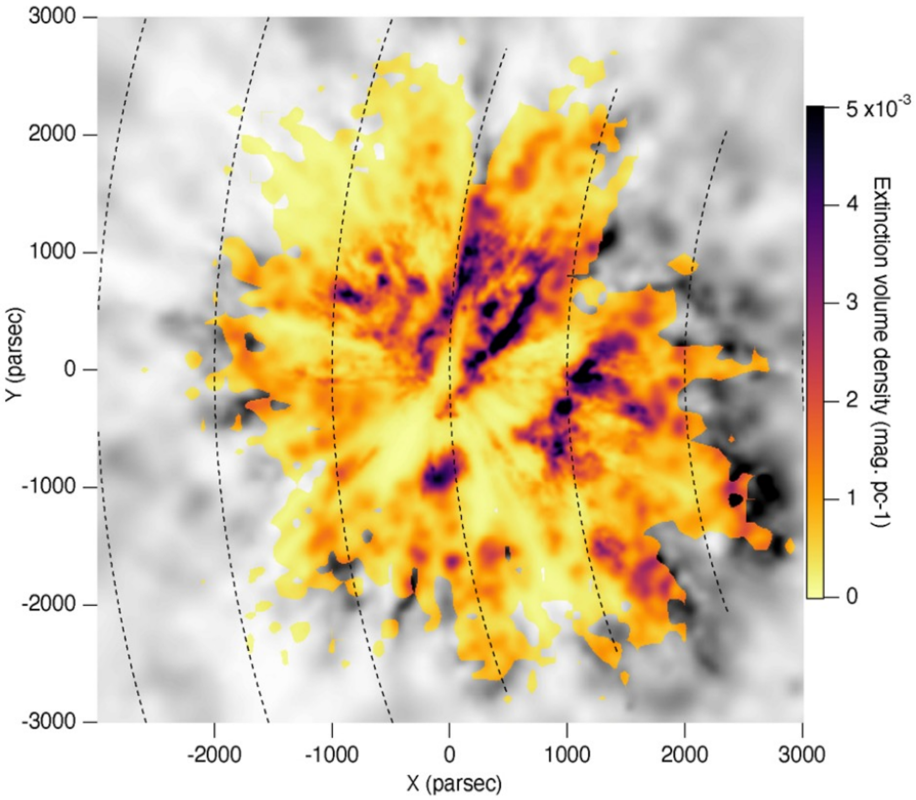

*

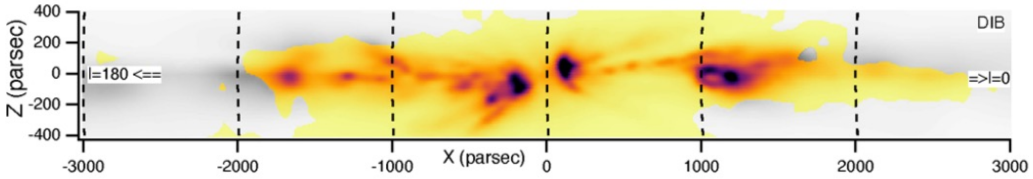

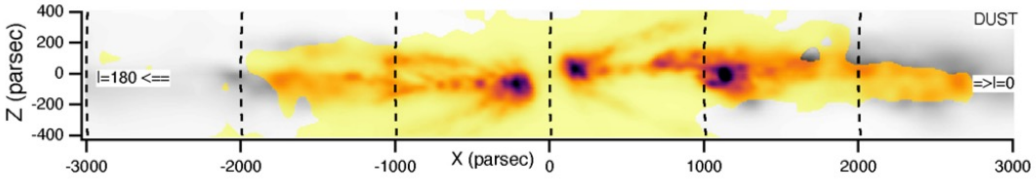

The visual comparison between the DIB and dust distributions using these figures reveals a very strong similarity, namely: regions with high dust density are characterized by a high DIB carrier density, and, reciprocally, regions with very low dust density are also characterized by very low DIB density.

4.1

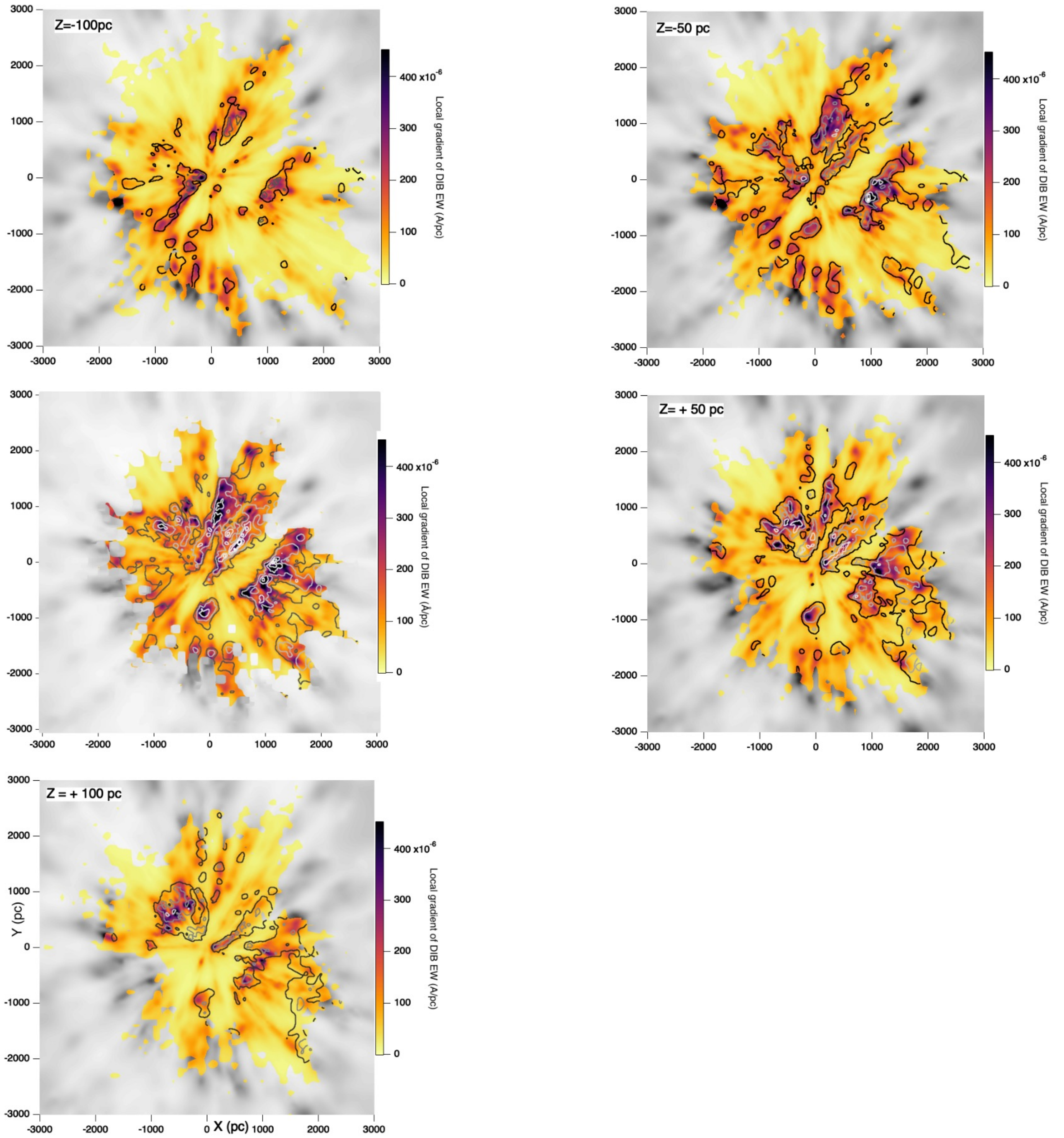

Fig. 5. 862.1 nm DIB carrier volume density in planar surfaces parallel to the Galactic disk and at different heights: –100, –50, 0, +50 and +100 pc. The extinction density iso-contours in the same surfaces for densities 1, 2, 4, 6, 8 × 10^{-3} mag pc^{-1} are superimposed.

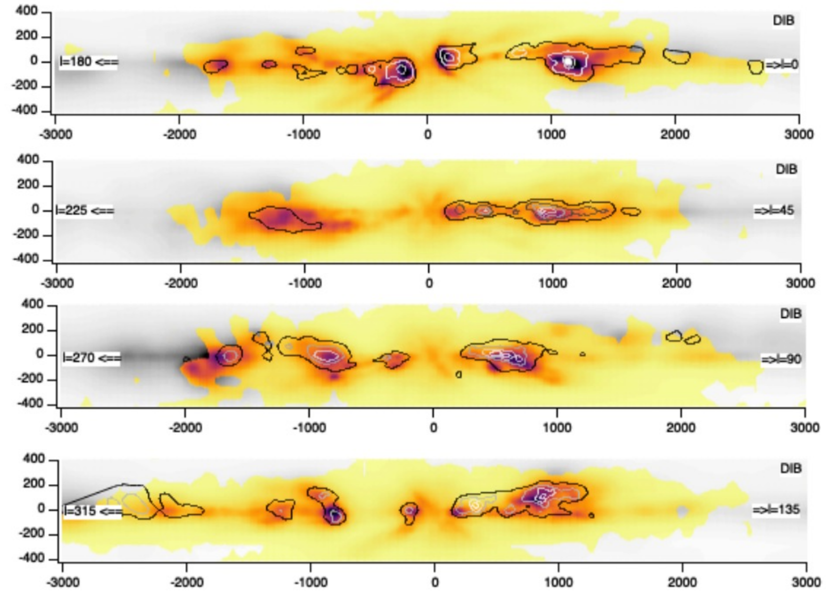

Fig. 6. Same as Fig. 5 for planar surfaces perpendicular to the Galactic disk and containing the Sun, oriented along various longitudes: 0–180°, 45–225°, 90–270°, and 135–315°. The extinction density iso-contours in the same surfaces for densities $1, 2, 4, 6, 8 \times 10^{-3}$ mag pc^{-1} are superimposed.

Comparison of the DIB and dust distributions in these maps shows very strong similarities, with areas of high dust density characterized by high DIB carrier density and areas of very low dust density also characterized by very low DIB density.

4. Results

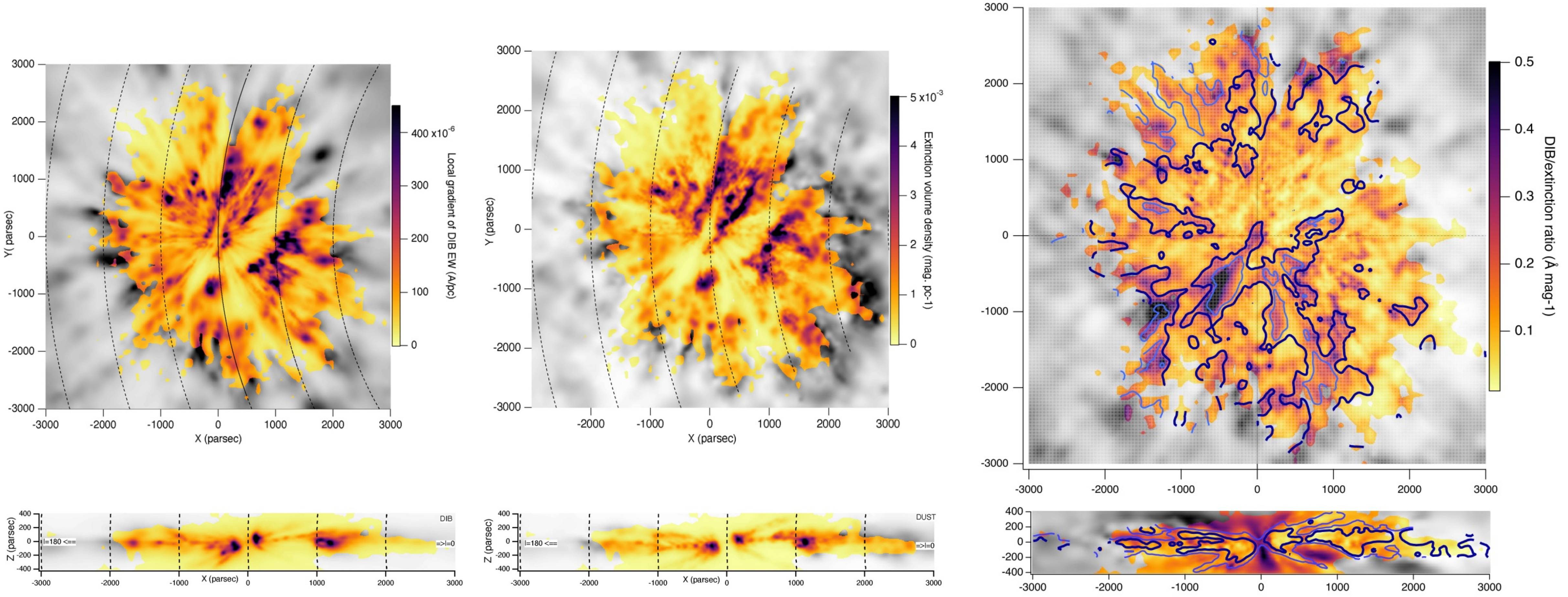

Fig. 7. Local values of the ratio between the DIB carrier volume density as measured by the EW local spatial gradient (in units of Å pc^{-1}) and the extinction volume density (in units of mag pc^{-1}). The two DIB-to-dust ratio maps are for the same planes as in Figs. 3 and 4. Iso-contours of extinction density for two low values (10^{-5} (black) and 5×10^{-4} (violet) mag pc^{-1}) are superimposed.

4. Results

- Figure 9 shows mean values of the DIB density, the extinction density, and their ratio, averaged in cylindric shells centred on the Galactic Center (GC), each of a galactocentric distance interval of 200 pc.
- An increase of the O-rich dust with respect to the C-rich dust in the inner Galaxy and closer to the Galactic plane.

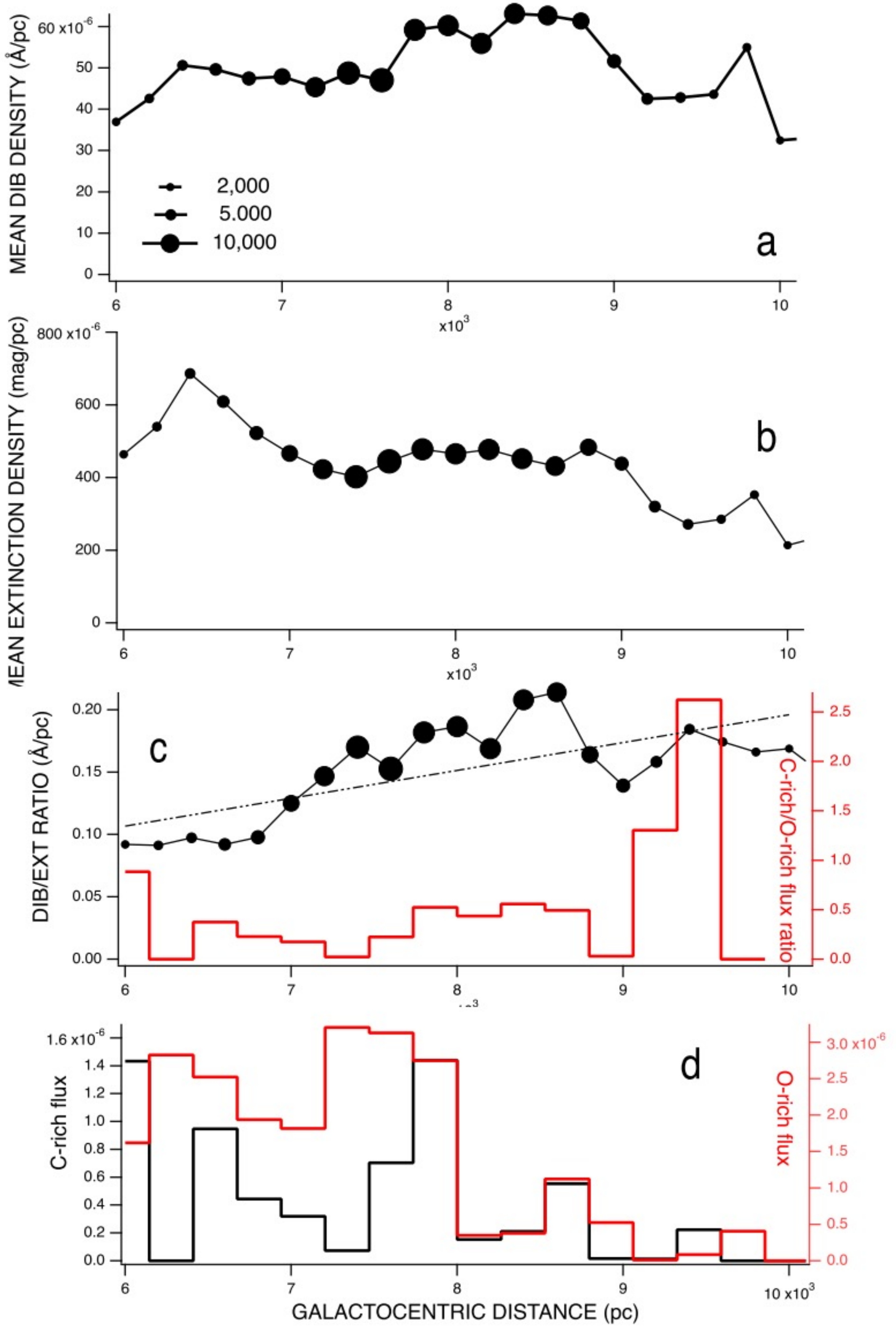

4. Results

- They computed the C-rich to O-rich dust flux ratio as a function of Z in 25 pc wide vertical slices, using the same catalog from Scicluna et al. (2022).
- There is a larger C/O ratio below the plane (from Z = −150 to Z = 0 pc) than above (between Z = 0 and Z = +150 pc), with a maximum at Z ≃ −50 pc.
- In case, this preponderance of C-rich dust at negative latitudes has an effect on the DIB density and will result in an increase of the DIB to dust ratio below the Plane; in turn, this leads to a shift of its minimum towards positive altitudes(the minimum is found at +50 pc).

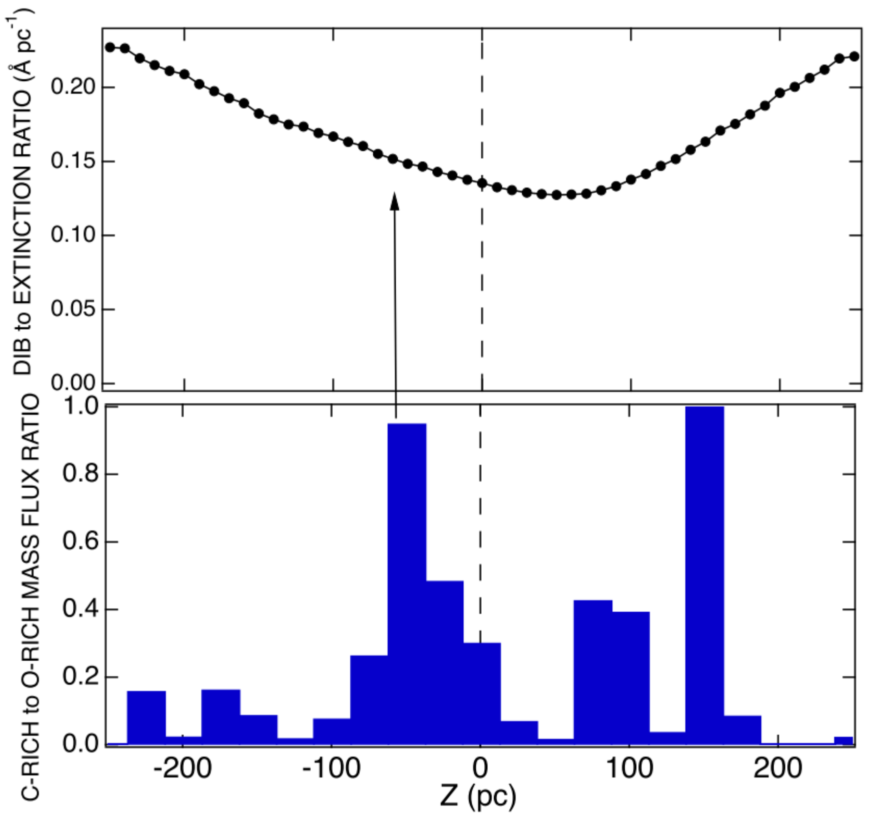

Fig. 10. Average values of the DIB to extinction density ratio in δZ = 10 pc horizontal slices as a function of the altitude Z (top). Ratio between C-rich and O-rich dust fluxes from AGBs, computed based on the catalog of Scicluna et al. (2022) for stars located in 25 pc wide horizontal slices (bottom).

Conclusion

- They used the recently published catalog of 862 nm DIB equivalent width measurements for individual stars, as well as corresponding Gaia positions and distances, to produce a 3D map of the DIB carrier density, using a hierarchical Bayesian inversion technique.
- The visual comparison between the 3D maps of DIB and dust reveals a very strong similarity, namely, regions filled with dust responsible for strong (resp. weak) optical extinction are characterized by a high (resp. low) DIB carrier density.
- They averaged densities and ratios in cylindric shells whose axes are vertical and contain the GC, for various galactocentric distances and found that the DIB to dust ratio is increasing radially (see Fig. 9).
- They used the catalog of Scicluna et al. (2022) and inferred that the production of C-rich dust is increasing radially by comparison with O-rich dust, in agreement with the direction of the DIB to dust gradient we observe here.
- While their results are still limited by the map resolution and ought to be confirmed in future works, the potential link they find with C-rich AGB stars show that full 3D mapping of DIB absorption data opens the way to new diagnostics about the processes involving their carriers.